

# Truncated denitrifiers dominate the denitrification pathway in tundra soil metagenomes

Igor S. Pessi<sup>1,2</sup>, Sirja Viitamäki<sup>1</sup>, Eeva Eronen-Rasimus<sup>1,3</sup>, Tom O. Delmont<sup>4</sup>,  
Miska Luoto<sup>5</sup> and Jenni Hultman<sup>1,2,\*</sup>

<sup>1</sup>Department of Microbiology, University of Helsinki, Finland

<sup>2</sup>Helsinki Institute of Sustainability Science (HELSUS), Finland

<sup>3</sup>Finnish Environment Institute (SYKE), Helsinki, Finland

<sup>4</sup>Department of Bioinformatics, Genoscope, Paris, France

<sup>5</sup>Department of Geosciences and Geography, University of Helsinki, Finland

\*Corresponding author: [jenni.hultman@helsinki.fi](mailto:jenni.hultman@helsinki.fi)

## Abstract

**In contrast to earlier assumptions, there is now mounting evidence for the role of tundra soils as important sources of the greenhouse gas nitrous oxide (N<sub>2</sub>O). However, the microorganisms involved in the cycling of N<sub>2</sub>O in these soils remain largely uncharacterized. In this study, we manually binned and curated 541 metagenome-assembled genomes (MAGs) from tundra soils in northern Finland. We then searched for MAGs encoding enzymes involved in denitrification, the main biotic process driving N<sub>2</sub>O emissions. Denitrifying communities were dominated by poorly characterized taxa with truncated denitrification pathways, i.e. lacking one or more denitrification genes. Among these, MAGs with the metabolic potential to produce N<sub>2</sub>O comprised the most diverse functional group. Re-analysis of a previously published metagenomic dataset from soils in northern Sweden supported these results, suggesting that truncated denitrifiers are dominant throughout the tundra biome.**

## Introduction

Nitrous oxide (N<sub>2</sub>O) is a potent greenhouse gas (GHG) that has approximately 300 times the global warming potential of carbon dioxide on a 100-year scale<sup>1</sup>. Despite being nitrogen (N) limited and enduring low temperatures throughout most of the year, tundra soils are increasingly recognized as important sources of N<sub>2</sub>O<sup>2-5</sup>. The relative contribution of tundra soils

30 to global GHG emissions is predicted to increase in the future<sup>6,7</sup>, as the warming rates  
31 experienced by high latitudes environments have been – and will likely continue to be – more  
32 than twice as high than in tropical and temperate regions<sup>8</sup>.

33 The main biotic control on N<sub>2</sub>O emissions is denitrification, which – like other biogeochemical  
34 cycles – is largely a microbial process<sup>9</sup>. Denitrification is a series of enzymatic steps in which  
35 nitrate (NO<sub>3</sub><sup>-</sup>) is sequentially reduced to nitrite (NO<sub>2</sub>), nitric oxide (NO), N<sub>2</sub>O, and dinitrogen  
36 (N<sub>2</sub>). The denitrification trait is found across a wide range of archaea, bacteria, and fungi, most  
37 of which are facultative anaerobes that switch to N oxides as electron acceptors in anoxic  
38 conditions<sup>10</sup>. Approximately only one-third of the genomes from cultured denitrifiers sequenced  
39 to date encode the full set of enzymes needed for complete denitrification<sup>11</sup>. Thus, at the  
40 ecosystem level, denitrification is often a community effort performed by different microbial  
41 populations that each execute a part of the process<sup>10,12</sup>.

42 Compared to high N<sub>2</sub>O-emitting systems (e.g. agricultural and tropical soils), our knowledge of  
43 denitrifying communities in tundra soils is poor. As denitrification ultimately leads to the loss  
44 of N to the atmosphere, it enhances the N-limited status of tundra systems thus impacting  
45 microbial and plant productivity<sup>13,14</sup>. Investigations of denitrifier diversity in the tundra have  
46 been largely limited to gene-centric surveys using microarrays, amplicon sequencing, qPCR,  
47 and read-based metagenomics, which provide limited information on the taxonomic identity and  
48 genomic composition of community members<sup>15–18</sup>. A better knowledge of the ecological,  
49 metabolic, and functional traits of denitrifiers is critical for improving current models and  
50 mitigating N<sub>2</sub>O emissions<sup>19</sup>. This invariably relies on the characterization of the so-called  
51 uncultured majority, i.e. microorganisms that have not been cultured to date and comprise a  
52 high proportion of the microbial diversity in complex ecosystems<sup>20,21</sup>. Genome-resolved  
53 metagenomics is a powerful tool to access the genomes of uncultured microorganisms and has  
54 provided important insights into carbon cycling processes in tundra soils<sup>22–24</sup>. However, this  
55 approach has not yet been applied to investigate the mechanisms driving N<sub>2</sub>O cycling in the  
56 tundra.

57 Here, we used genome-resolved metagenomics to investigate the diversity and genomic  
58 composition of potential denitrifiers in tundra soils. By leveraging two comprehensive  
59 metagenomic datasets of Finnish and Swedish soils, we show that tundra denitrifying  
60 communities are dominated by microorganisms with truncated denitrification pathways, i.e.  
61 harbouring only a subset of the enzymes required for complete denitrification. Non-denitrifying  
62 N<sub>2</sub>O-producers were the most diverse group and included many members of the phylum  
63 Acidobacteriota, a ubiquitous group in soils worldwide with a low representation in culture

64 collections. In contrast with earlier estimates based on genomes from cultured  
65 microorganisms<sup>11</sup>, our genome-resolved metagenomics survey allowed access to the genomes of  
66 poorly characterized taxa and revealed that, within a defined ecosystem, the proportion of  
67 genomes encoding the complete denitrification pathway can be as low as 1%.

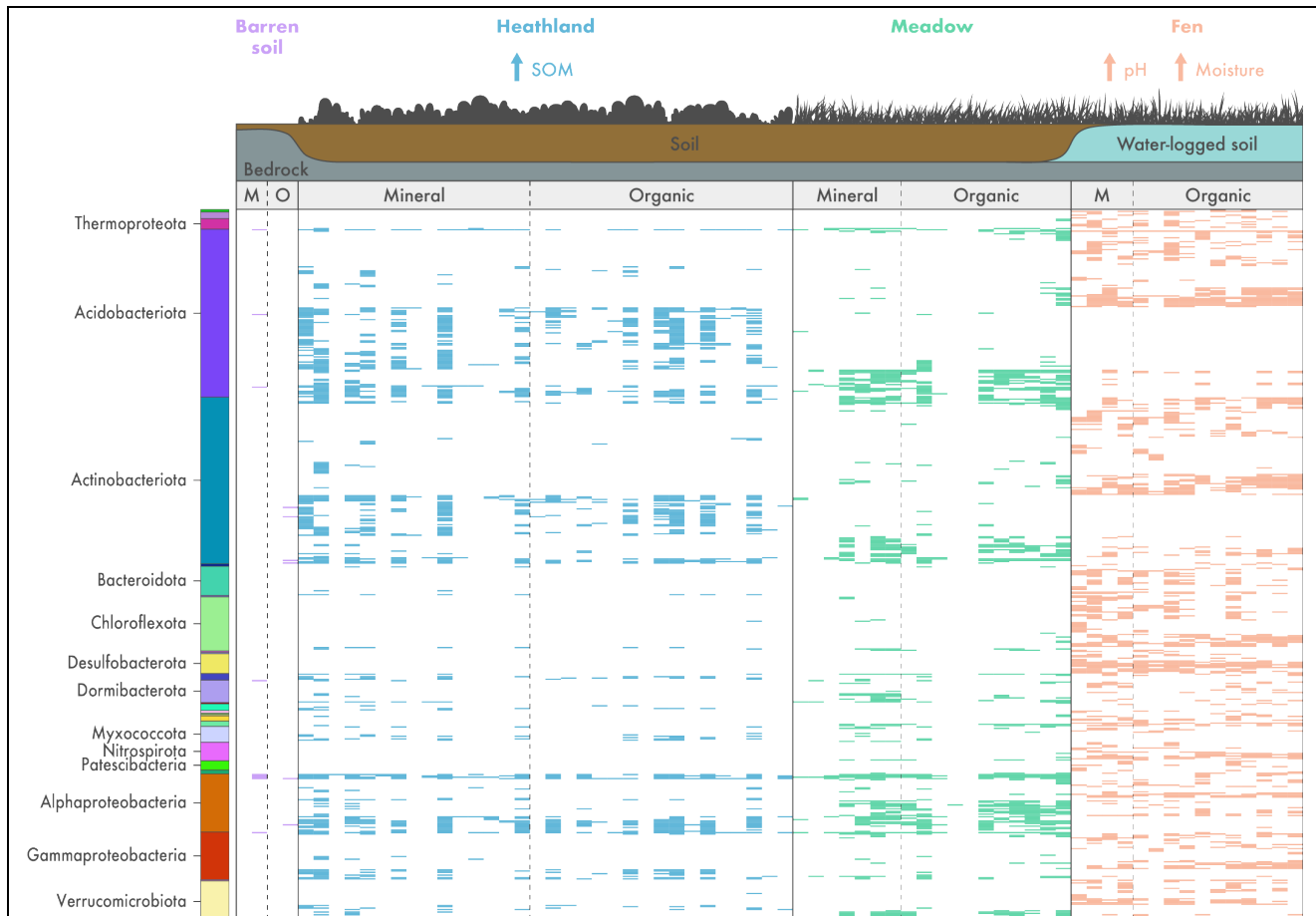
## 68 **Results**

### 69 **A manually curated genomic database from tundra soil metagenomes**

70 We analysed more than 9 billion Illumina (1.4 Tb) and 7 million Nanopore reads (21.5 Gb) from  
71 69 soil metagenomes sampled in an area of mountain tundra biome in Kilpisjärvi, northern  
72 Finland (**Suppl. Fig. S1, Suppl. Table S1**). In previous studies, we have established in the  
73 area a systematic fine-scale sampling of microclimate, soil conditions, and vegetation in  
74 topographically distinct habitats<sup>25–27</sup>. Local variation in topography and soil properties creates  
75 a mosaic of habitats characterized by contrasting ecological conditions (e.g. microclimate,  
76 vegetation productivity, cover, and biomass). This makes the study setting ideal to investigate  
77 biotic interactions and species-environment relationships in tundra ecosystems<sup>27–29</sup>. Our  
78 sampling design included two soil depths across four ecosystems that are characteristic of polar  
79 and alpine environments (barren soils, heathlands, meadows, and fens). Soil ecosystems differ  
80 in vegetation cover and physicochemical composition, with fens in particular being  
81 characterized by higher pH and moisture content (**Suppl. Fig. S1**). Microbial community  
82 composition also differs, with fen soils harbouring contrasting microbial communities compared  
83 to the other ecosystems (**Suppl. Fig. S2**).

84 Two Illumina co-assemblies and two individual Nanopore assemblies yielded nearly 20 million  
85 contigs longer than 1,000 bp, with a total assembly size of 50.0 Gb. Using anvi'o<sup>30</sup>, we obtained  
86 3,257 genomic bins and manually curated these to a set of 539 unique metagenome assembled  
87 genomes (MAGs) (**Fig. 1, Suppl. Fig. S3, Suppl. Fig. S4, Suppl. Table S2**). On average, 8.6%  
88 of the reads from each sample were recruited by the MAGs (minimum: 2.7%, maximum: 22.4%).  
89 According to estimates based on domain-specific single-copy genes, the obtained MAGs are on  
90 average 67.7% complete (50.7–100.0%) and 2.5% redundant (0.0–9.9%) (**Suppl. Table S2**).  
91 Phylogenomic analyses based on 122 archaeal and 120 bacterial single-copy genes in the context  
92 of the Genome Taxonomy Database (GTDB)<sup>31,32</sup> placed the Kilpisjärvi MAGs across a diverse  
93 range of bacterial and archaeal phyla, including Acidobacteriota (n = 127), Actinobacteriota  
94 (n = 126), Alphaproteobacteria (n = 44), Chloroflexota (n = 41), Gammaproteobacteria (n = 36),  
95 and Verrucomicrobiota (n = 31) (**Fig. 1, Suppl. Fig. S3**). Of the 541 MAGs, only 78 were

96 assigned to a validly described genera (**Suppl. Table S2**). Most MAGs ( $n = 463$ ) belong to  
97 genera that do not comprise formally described species. These include 183 MAGs that were  
98 placed outside genus-level lineages currently described in GTDB and thus likely represent novel  
99 genera.



100 **Fig. 1 | Genome-resolved metagenomics of microorganisms in tundra soils.** Detection  
101 profile of 539 metagenome-assembled genomes (MAGs) recovered from mineral and organic  
102 soils across different ecosystems in Kilpisjärvi, northern Finland. A MAG was detected in a  
103 given sample if  $\geq 50\%$  of its nucleotides had  $\geq 1x$  coverage. Phylum-level taxonomic assignments  
104 are shown only for the major groups found. A complete representation of all phyla can be found  
105 in **Suppl. Fig. S3** and additional information about the MAGs is provided in **Suppl. Table S2**.

106 The highest number of MAGs ( $n = 341$ ) was detected in the fen soils (**Suppl. Fig. S4**). Although  
107 barren and fen soils had similar taxonomic richness according to gene-centric estimates (**Suppl.**  
108 **Fig. S2**), the genome-resolved approach recovered only a small fraction of the microbial  
109 diversity in barren soils ( $n = 15$ ). This is likely a result of limited sampling and sequencing of  
110 this ecosystem (**Suppl. Table S1**). The number of detected MAGs in heathland and meadow  
111 soils was similar ( $n = 223$  and  $n = 217$ , respectively) (**Suppl. Fig. S4**). In agreement with the

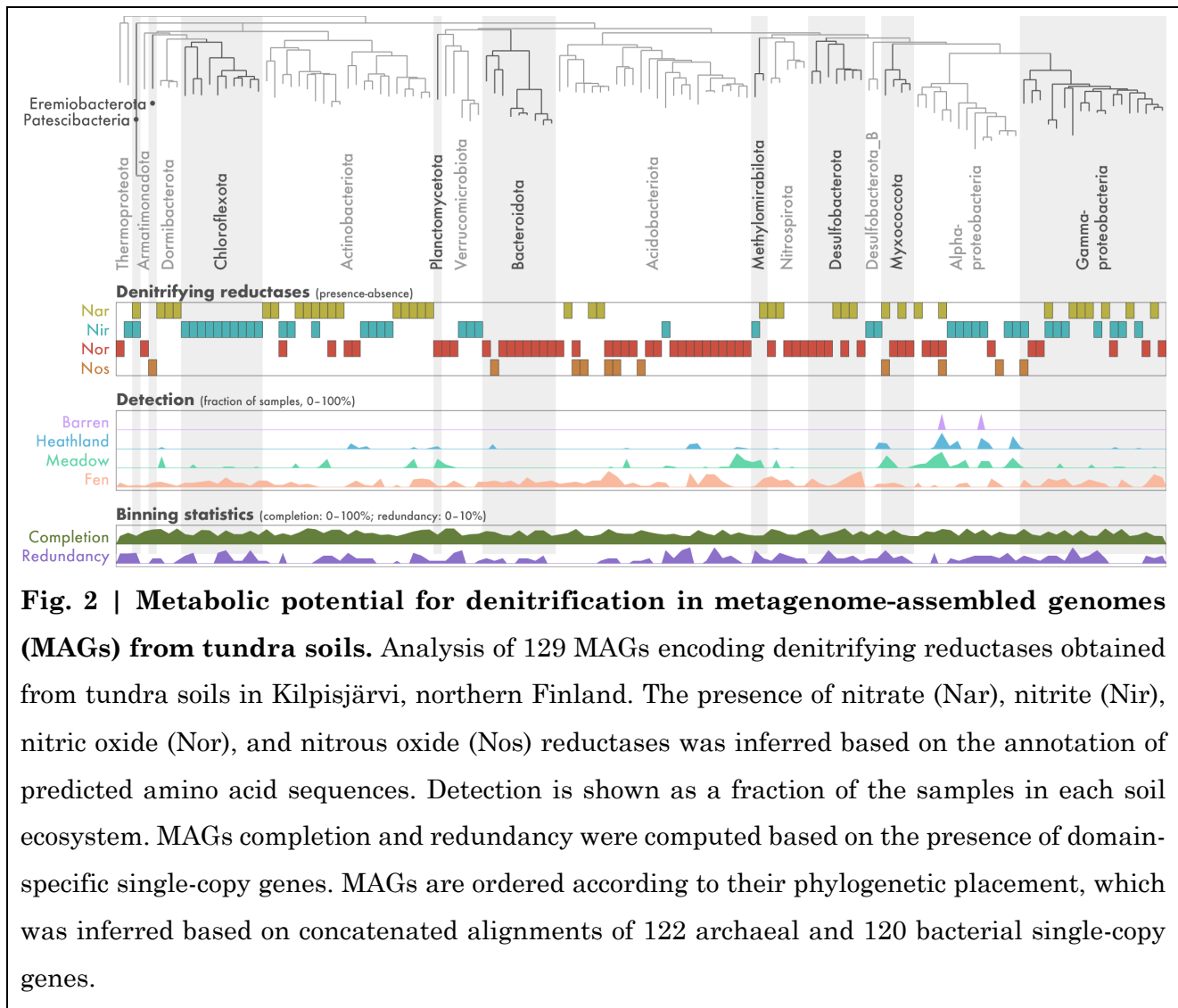
112 gene-centric assessment (**Suppl. Fig. S2**), we observed differences in MAG composition across  
113 the soil ecosystems (**Suppl. Fig. S4**). Only 41 MAGs (7.6%) were shared between the heathland  
114 and fen soils. On the other hand, meadow communities represent an intermediate state between  
115 heathland and fens, sharing 115 and 125 MAGs with these ecosystems, respectively. This is  
116 likely a reflection of edaphic similarities between the ecosystems (**Suppl. Fig. S1**). Meadow  
117 soils have similar moisture levels to heathlands but, as fens, have graminoid plants as the  
118 dominant vegetation cover.

## 119 **MAGs from tundra soils have truncated denitrification pathways**

120 To gain insights into the microorganisms involved with the cycling of N<sub>2</sub>O in tundra soils, we  
121 annotated the predicted amino acid sequences of the Kilpisjärvi MAGs across a range of protein  
122 databases (COG<sup>33</sup>, KEGG<sup>34</sup>, KOfam<sup>35</sup>, RefSeq<sup>36</sup>, and Swiss-Prot<sup>37</sup>). We then searched for MAGs  
123 with a metabolic potential for denitrification, the main process controlling N<sub>2</sub>O production in  
124 soils<sup>9</sup>. The complete denitrification pathway is performed by microorganisms containing the  
125 *narG/napA*, *nirK/nirS*, *norB*, and *nosZ* genes, which encode the nitrate (Nar), nitrite (Nir), nitric  
126 oxide (Nor), and nitrous oxide (Nos) reductases, respectively<sup>10</sup>. In the Kilpisjärvi soils, the  
127 metabolic potential for denitrification was exclusively restricted to MAGs with truncated  
128 denitrification pathways, i.e. MAGs missing one or more denitrifying reductases (**Fig. 2**). Of the  
129 129 MAGs harbouring denitrifying reductases, 114 contain only one of the four enzymes and no  
130 MAG encode all the Nir, Nor, and Nos enzymes required for complete denitrification, i.e. the  
131 reduction of NO<sub>2</sub><sup>-</sup> to N<sub>2</sub>. MAGs encoding denitrifying reductases were detected mainly in the  
132 meadow and fen soils, where the abundance of denitrification genes was the highest (**Suppl.**  
133 **Fig. S2**). MAGs belong to the archaeal phylum Thermoproteota and many bacterial phyla such  
134 as Gamma- and Alphaproteobacteria, Acidobacteriota, Bacteroidota, Actinobacteriota, and  
135 Chloroflexota (**Fig. 2**). Only 19 MAGs were assigned to a validly described genera (**Suppl.**  
136 **Table S2**).

137 Truncated pathways do not appear to be a methodological artifact arising from the metabolic  
138 reconstruction of fragmented genomes. Indeed, truncated denitrifiers include 23 high-quality  
139 MAGs (≥ 90% complete) and no relationship was observed between the number of denitrifying  
140 reductases encoded by the MAGs and their estimated completion values (**Suppl. Fig. S5**). To  
141 verify if microorganisms with truncated denitrification pathways are common in other tundra  
142 systems, we expanded our analysis to 1529 MAGs recovered from permafrost peatland, bog, and  
143 fen soils in Stordalen Mire, northern Sweden<sup>24</sup>. Annotation and metabolic reconstruction of the  
144 Stordalen Mire MAGs corroborated the observations from Kilpisjärvi MAGs (**Suppl. Fig. S6**).  
145 The distribution of denitrifying reductases was remarkably similar in MAGs from both systems,

146 and MAGs with truncated denitrification pathways were also the norm in Stordalen Mire soils.  
147 Of the 396 Stordalen Mire MAGs encoding denitrifying reductases, only six harbour all the Nir,  
148 Nor, and Nos enzymes required for complete denitrification. Altogether, the analysis of these  
149 two comprehensive datasets suggest that microorganisms with truncated denitrification  
150 pathways are widespread throughout tundra ecosystems.



## 160 Fen soils harbour Chloroflexota MAGs with divergent Nir enzymes

161 The reduction of  $\text{NO}_2^-$  to  $\text{NO}$ , performed by microorganisms containing the Nir enzyme, is the  
162 hallmark step of denitrification and is often referred to as denitrification *stricto sensu*, as it  
163 involves the conversion of a soluble substrate to a gaseous product thus leading to the removal  
164 of N from the system<sup>10</sup>. Within the 129 Kilpisjärvi MAGs encoding denitrifying reductases, 41  
165 are potential denitrifiers *stricto sensu* (**Fig. 2**). Most MAGs (n = 38) harbour the copper-  
166 containing form of Nir encoded by the *nirK* gene. The cytochrome *cd1*-containing form of Nir

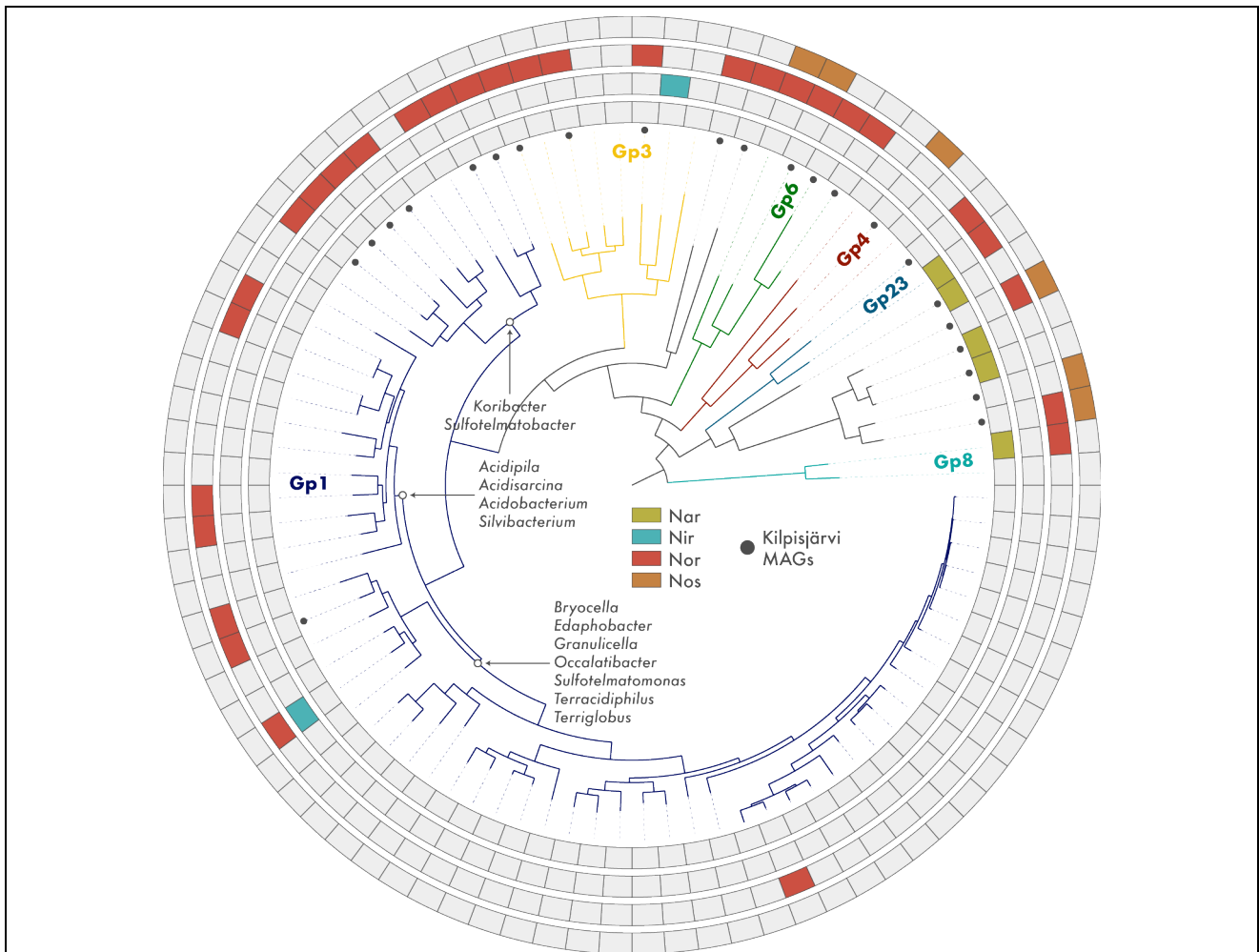
167 encoded by the *nirS* gene was found in four Gammaproteobacteria MAGs, including one MAG  
168 that encodes both forms of the enzyme. Most Nir-encoding MAGs belong to the bacterial phyla  
169 Alpha- and Gammaproteobacteria, Chloroflexota, and Actinobacteriota (**Fig. 2**). Denitrifying  
170 *stricto sensu* communities differed between the meadow and fen soils (**Suppl. Figure S7a**).  
171 Alphaproteobacteria comprised half of the Nir-encoding MAGs in the meadow soils, while  
172 Chloroflexota and Gammaproteobacteria were the majority in the fens. Interestingly, the amino  
173 acid sequence composition of the Nir enzymes from Chloroflexota MAGs were quite divergent  
174 (**Suppl. Figure S7b**). These had lower identity with reference sequences from RefSeq  
175 (31.6–66.3%) than the sequences of MAGs from better characterized phyla such as the Alpha-  
176 and Gammaproteobacteria (67.5–88.8% and 76.3–91.7%, respectively). Indeed, most Nir-  
177 encoding Chloroflexota MAGs were assigned to the class-level lineage Ellin6529 (**Suppl. Table**  
178 **S2**), a major group in soils worldwide that at present does not include cultured  
179 representatives<sup>38</sup>.

## 180 **The potential for N<sub>2</sub>O production is widespread among the Acidobacteriota**

181 The stepwise reduction of NO to N<sub>2</sub>O and N<sub>2</sub> catalysed by the Nor and Nos enzymes represents  
182 the final step of denitrification and the main biotic control on N<sub>2</sub>O emissions. Soil denitrification  
183 rates depend on multiple environmental conditions such as adequate moisture and inorganic N  
184 availability, but whether it results in the emission of N<sub>2</sub>O or N<sub>2</sub> is ultimately linked to a balance  
185 between the activity of NO and N<sub>2</sub>O reducers<sup>9</sup>. Kilpisjärvi MAGs with a metabolic potential for  
186 NO and N<sub>2</sub>O reduction (n = 56 and n = 11, respectively) are almost exclusively non-denitrifiers  
187 *stricto sensu*, i.e. they do not encode the Nir enzyme involved in the reduction of NO<sub>2</sub><sup>-</sup> to NO  
188 (**Fig. 2**). Only four MAGs encode both Nor and Nos and thus have the potential to reduce NO  
189 completely to N<sub>2</sub>. Most MAGs with potential NO-reducing capability (n = 48) contain the qNor  
190 enzyme encoded by the *norB* gene, which is a monomeric form of Nor found in denitrifying  
191 bacteria and archaea and non-denitrifying pathogenic bacteria<sup>39</sup>. The remaining MAGs (n = 8)  
192 harbour the cytochrome c-dependent form of Nor (cNor) encoded by *norBC*.

193 MAGs with the potential to reduce NO to N<sub>2</sub>O were particularly prominent among the phylum  
194 Acidobacteriota (n = 18 MAGs) (**Fig. 2**), an ubiquitous group in tundra and other soil ecosystems  
195 worldwide<sup>38,40</sup>. Acidobacteriota are very recalcitrant to culturing efforts. Of the 26 subdivisions  
196 identified by 16S rRNA gene surveys, only seven contain genera that have been properly  
197 described based on cultured representatives<sup>41</sup>. Our analysis of MAGs from tundra soils and all  
198 available genomes of Acidobacteriota strains and candidate taxa suggests that the potential for  
199 NO reduction to N<sub>2</sub>O is widespread within members of this phylum (**Fig. 3**). Potential N<sub>2</sub>O  
200 producers are particularly prominent in the subdivisions Gp1, Gp3, and Gp23, including the

201 genera *Sufotelmatomonas*, *Acidobacterium*, *Silvibacterium*, *Sulfotelmatobacter*, *Koribacter*, and  
202 *Thermoanaerobaculum*. On the other hand, genomes with potential to reduce NO completely to  
203 N<sub>2</sub> are mostly found in the subdivision Gp6 (including the strain *Luteitalea pratensis* DSM  
204 100886) and in an early-branching subdivision without cultured representatives related to Gp23  
205 (Fig. 3). This clade includes the Kilpisjärvi MAG KWL-0326, an abundant member of the  
206 tundra communities detected in all fens and half of the meadow samples at relative abundances  
207 of up to nearly 1% (Suppl. Fig. S4).



208 **Fig. 3 | Metabolic potential for denitrification in members of the phylum**  
209 **Acidobacteriota.** Phylogenomic analysis of 23 Acidobacteriota MAGs encoding denitrifying  
210 reductases recovered from tundra soils in Kilpisjärvi, northern Finland, and 64 published  
211 genomes of Acidobacteriota strains and candidate taxa. Maximum likelihood tree based on  
212 concatenated alignments of 23 ribosomal proteins and rooted with *Escherichia coli* ATCC 11775  
213 (not shown). The presence of nitrate (Nar), nitrite (Nir), nitric oxide (Nor), and nitrous oxide  
214 (Nos) reductases was inferred based on the annotation of predicted amino acid sequences.



## 215 Discussion

216 The 539 MAGs obtained in the present study by a manual binning and curation effort represent  
217 one of the largest genomic catalogues of microorganisms from tundra soils to date (**Fig. 1,**  
218 **Suppl. Fig. S3, Suppl. Fig. S4, Suppl. Table S2**). Our dataset is comparable to a previous  
219 metagenomic investigation of soils in Stordalen Mire, northern Sweden, which included 647  
220 unique MAGs obtained from 1.7 Tb of metagenomic data<sup>24</sup>. Here, we leveraged these two  
221 comprehensive datasets to investigate the genomic makeup of microorganisms involved with  
222 denitrification in tundra soils, with the ultimate goal of gaining insights into mechanisms of  
223 N<sub>2</sub>O emission from these systems. Our results strongly indicate that tundra soils are dominated  
224 by microorganisms with truncated denitrification pathways, most of which represent poorly  
225 characterized taxa without cultured representatives (**Fig. 2, Suppl. Fig. S5, Suppl. Fig. S6,**  
226 **Suppl. Fig. S7**). Unlike well-known denitrifiers such as *Bradyrhizobium japonicum*<sup>42,43</sup>, our  
227 genome-resolved metagenomics survey indicates that dominant microbial populations in tundra  
228 soils do not have the metabolic potential for complete denitrification. Instead, the potential for  
229 denitrification in tundra soils is highly modular, with each step of the pathway (NO<sub>3</sub><sup>-</sup>, NO<sub>2</sub><sup>-</sup>,  
230 NO, and N<sub>2</sub>O reduction) encoded by different microbial populations.

231 It has been suggested that denitrification is a community process performed in synergy by  
232 different microbial taxa that execute only a subset of the complete denitrification pathway<sup>10,12</sup>.  
233 With the growing number of microbial genomes sequenced in recent decades, it became evident  
234 that only a fraction of the microorganisms involved in the denitrification pathway encode the  
235 enzymatic machinery needed for complete denitrification<sup>11,42,43</sup>. For instance, in a study that  
236 included 652 genomes of cultured microorganisms harbouring denitrifying reductases retrieved  
237 from GenBank, Graf et al.<sup>11</sup> found that only approximately 31% are complete denitrifiers.  
238 However, the magnitude of truncated denitrification pathways found in our dataset of tundra  
239 metagenomes was much more pronounced. Our genome-resolved metagenomics approach  
240 enabled us to access to the genomes of uncultured, poorly characterized taxa, which comprise  
241 the majority of the microorganisms in soils and other complex ecosystems<sup>20,21</sup>. By expanding the  
242 genomic catalogue of denitrifiers to include uncultured taxa, our results revealed a higher  
243 magnitude of truncated denitrification pathways than previous assessments based on genomes  
244 from cultured microorganisms. Moreover, from an ecosystem perspective, the contribution of  
245 microorganisms with truncated denitrification pathways has been largely overlooked. In tundra  
246 systems in particular, earlier investigations applying a gene-centric approach have shown that  
247 the potential for complete denitrification is present within defined microbial communities<sup>44,45</sup>.  
248 However, gene-centric approaches fail to reveal the wider genomic context in which these genes

249 are inserted. By applying the genome-resolved metagenomics approach, we traced  
250 denitrification genes to specific microbial populations, thereby allowing a detailed investigation  
251 of the genomic makeup of potential denitrifiers in tundra soils. In addition to their  
252 predominance in genomic databases<sup>11</sup>, our genome-resolved metagenomics survey revealed that  
253 truncated denitrifiers are also dominant within a defined ecosystem.

254 Microorganisms harbouring the Nor enzyme – and thus with the potential to reduce NO to N<sub>2</sub>O  
255 – were the most diverse functional group and were particularly prominent among the phylum  
256 Acidobacteriota (**Fig. 3**). Members of this phylum, which comprise mostly oligotrophic (k-  
257 strategist) taxa, make up an important fraction of the microbial communities in polar and alpine  
258 soils<sup>38,40</sup>. Earlier genomic investigations have identified denitrifying reductases within  
259 Acidobacteriota genomes, but have disregarded their potential role in denitrification due to the  
260 presence of truncated pathways<sup>46,47</sup>. The potential contribution of Acidobacteriota to the soil  
261 denitrification process in tundra soils is supported by other studies that have shown that,  
262 despite not having a complete denitrification machinery, truncated denitrifiers can contribute  
263 to *in situ* processes<sup>43,48–51</sup>. For example, Lycus et al.<sup>48</sup> applied an elegant cultivation approach  
264 using different N oxides as sole electron acceptors and isolated a wide diversity of  
265 microorganisms with different types of truncated denitrification pathways that are able to grow  
266 on single N oxides. These included, for instance, microorganisms that can grow using NO as an  
267 electron acceptor generating N<sub>2</sub>O but are unable to perform any other step of the denitrification  
268 process. Moreover, studies have suggested that incomplete denitrifiers that contain Nir and Nor  
269 but lack Nos (thus having N<sub>2</sub>O as the end product of denitrification) can contribute substantially  
270 to soil N<sub>2</sub>O emissions<sup>49</sup>. At the same time, non-denitrifying N<sub>2</sub>O reducers, microorganisms that  
271 contain Nos but lack Nir, can represent an important N<sub>2</sub>O sink<sup>43,50,51</sup>.

272 A great challenge in microbial ecology has been to link microbial community structure to  
273 biogeochemical processes<sup>52</sup>. While microorganisms with truncated denitrification pathways  
274 dominated the denitrifying communities investigated here, the potential for complete  
275 denitrification was indeed present at the ecosystem level. Our current knowledge of the  
276 regulation of the denitrification process is largely based on the activity of model organisms such  
277 as the complete denitrifier *Paracoccus denitrificans*<sup>53</sup>. It thus remains unclear how such a  
278 community dominated by truncated denitrifiers interacts with each other and the environment  
279 and impact N<sub>2</sub>O emissions *in situ*. A better understanding of the activity of truncated  
280 denitrifiers is paramount for our ability to model N<sub>2</sub>O emissions and mitigate climate  
281 change<sup>19,53</sup>. High-latitude environments in particular have experienced amplified warming in  
282 recent decades, a trend that is likely to continue in the coming centuries<sup>8</sup>. As mechanisms of  
283 GHG emissions are very climate sensitive, the contribution of tundra soils to global GHG

284 atmospheric levels is thus predicted to increase in the future leading to a positive feedback  
285 loop<sup>6,7</sup>. Compared with carbon dioxide and methane fluxes, measurements of N<sub>2</sub>O emissions in  
286 tundra soils are sparse, making the magnitude of N<sub>2</sub>O fluxes across the polar regions uncertain<sup>5</sup>.  
287 In addition to a better monitoring of N<sub>2</sub>O emissions throughout the tundra biome, our results  
288 suggest that a better understanding of the contribution of tundra soil to global N<sub>2</sub>O levels should  
289 include the investigation of the mechanisms of metabolic regulation in communities dominated  
290 by truncated denitrifiers.

## 291 **Methods**

### 292 **Study area and sampling**

293 The Saana Nature Reserve (69.04°N, 20.79°E) is located in Kilpisjärvi, northern Finland  
294 (**Suppl. Fig. S1a**). The area is part of the oroarctic mountain tundra biome, which is  
295 characterized by a mean annual temperature of  $-1.9^{\circ}\text{C}$  and annual precipitation of 487 mm<sup>54</sup>.  
296 Our study sites (n = 43) are distributed across Mount Saana and Mount Korkea-Jehkas and the  
297 valley in between and include four soil ecosystems: barren soils (n = 2), heathlands (n = 18),  
298 meadows (n = 7), and fens (n = 16) (**Suppl. Fig. S1b**). Sampling was performed in July 2017  
299 and July 2018, during the growing season in the northern hemisphere. Samples were obtained  
300 with a soil corer sterilized with 70% ethanol and, when possible, soil cores were split into organic  
301 and mineral samples using a sterilized spatula. In total, 41 organic and 28 mineral samples  
302 were obtained. Samples were transferred to a whirl-pack bag and immediately frozen in dry ice.  
303 Samples were transported frozen to the laboratory at the University of Helsinki and kept at  
304  $-80^{\circ}\text{C}$  until analyses.

### 305 **Metagenome sequencing**

306 Total DNA and RNA were co-extracted as previously described<sup>27</sup>. Briefly, extraction was  
307 performed on 0.5 g of soil using a hexadecyltrimethyl ammonium bromide (CTAB), phenol-  
308 chloroform, and bead-beating protocol. DNA was purified using the AllPrep DNA Mini Kit  
309 (QIAGEN, Hilden, Germany) and quantified using the Qubit dsDNA BR Assay Kit  
310 (ThermoFisher Scientific, Waltham, MA, USA). Library preparation for Illumina metagenome  
311 sequencing was performed using the Nextera XT DNA Library Preparation Kit (Illumina, San  
312 Diego, CA, USA). Metagenomes were obtained for 69 samples across two paired-end NextSeq  
313 (132–170 bp) and one NovaSeq (2 x 151 bp) runs. Two samples were additionally sequenced with  
314 Nanopore MinION. For this, libraries were prepared using the SQK-LSK109 Ligation

315 Sequencing Kit with the long fragment buffer (Oxford Nanopore Technologies, Oxford, UK) and  
316 the NEBNext Companion Module for Oxford Nanopore Technologies Ligation Sequencing Kit  
317 (New England Biolabs). Each sample was sequenced for 48 hours on one R9.4 flow cell.

## 318 **Processing of raw metagenomic data**

319 The quality of the raw Illumina data was verified with fastQC<sup>55</sup> v0.11.9 and multiQC<sup>56</sup> v1.8.  
320 Cutadapt<sup>57</sup> v1.16 was then used to trim 3' adapters and low-quality base calls ( $q < 20$ ) and to  
321 filter out short reads ( $< 50$  bp). Nanopore data were basecalled with GPU guppy v4.0.11 using  
322 the high-accuracy model and applying a minimum quality score of 7. The quality of the  
323 basecalled Nanopore data was assessed with pycoQC<sup>58</sup> v2.5.0.21 and adapters were trimmed  
324 with Porechop<sup>59</sup> v0.2.4.

## 325 **Gene-centric analyses**

326 Taxonomic and functional profiles of the microbial communities were obtained using a gene-  
327 centric approach based on unassembled Illumina data. Due to differences in sequencing depth  
328 across the samples, the dataset was resampled to 2,000,000 reads per sample with seqtk<sup>60</sup> v1.3.  
329 Taxonomic profiles were obtained by annotating SSU rRNA gene sequences against the SILVA  
330 database<sup>61</sup> release 111 with METAXA<sup>62</sup> v2.2. Functional profiles were obtained by blastx  
331 searches against the KEGG database<sup>34</sup> release 86 with DIAMOND<sup>63</sup> v0.9.14. Only matches with  
332 a maximum e-value of  $10^{-5}$  and minimum identity of 60% were considered. The KEGG Orthology  
333 (KO) identifier of the best hit was assigned to each read and KEGG modules were summarised  
334 with the package keggR<sup>64</sup> v0.9.1 in R. Gene relative abundances were normalized to the  
335 abundance of the *rpoB* gene. Differences in richness (i.e. the number of genera and functional  
336 genes in each sample) between the ecosystems were assessed using one-way analysis of variance  
337 (ANOVA) followed by Tukey's HSD test in R. The same test was performed to assess differences  
338 in the abundance of individual N cycle genes. Differences in taxonomic and functional  
339 community structure were assessed using non-metric multidimensional scaling (NMDS) and  
340 permutational ANOVA (PERMANOVA) with the package vegan<sup>65</sup> v2.5.6 in R.

## 341 **Metagenome assembling**

342 Metagenome assembling of the Illumina data was performed as two co-assemblies. One co-  
343 assembly was performed for the upland (barren, heathland, and meadow) and other for the fen  
344 samples. For each co-assembly, reads from the respective samples were pooled and assembled  
345 with MEGAHIT<sup>66</sup> v1.1.1.2. Assembling of the Nanopore data was done for each sample

346 individually with Flye<sup>67</sup> v2.7.1 in metagenome mode. Contigs were corrected based on Illumina  
347 data from the respective sample with bowtie<sup>68</sup> v2.3.5, SAMtools<sup>69</sup> v1.9, and pilon<sup>70</sup> v1.23. Quality  
348 assessment of the (co-)assemblies was obtained with metaQUAST<sup>71</sup> v5.0.2.

## 349 **Metagenome binning**

350 Binning was performed separately for each Illumina and Nanopore (co-)assembly with anvi'o<sup>30</sup>  
351 v6.2 after discarding contigs shorter than 2500 bp. Gene calls were predicted with prodigal<sup>72</sup>  
352 v2.6.3. Single-copy genes were identified with HMMER<sup>73</sup> v.3.2.1 and classified with  
353 DIAMOND<sup>63</sup> v0.9.14 against the GTDB<sup>31,32</sup> release 04-RS89. Illumina reads were mapped to the  
354 contigs with bowtie<sup>68</sup> v2.3.5 and SAM files were sorted and indexed using SAMtools<sup>69</sup> v1.9. Due  
355 to their large sizes, Illumina co-assemblies were split into 100 smaller clusters based on  
356 differential coverage and tetranucleotide frequency with CONCOCT<sup>74</sup> v1.0.0. Contigs were then  
357 manually sorted into bins based on the same composition and coverage metrics using the 'anvi-  
358 interactive' interface in anvi'o<sup>30</sup> v6.2. Nanopore contigs were binned directly without pre-  
359 clustering with CONCOCT. Bins that were  $\geq 50\%$  complete according to the presence of single-  
360 copy genes were further refined using the 'anvi-refine' interface in anvi'o<sup>30</sup> v6.2. In addition to  
361 taxonomic signal (based on single-copy genes classified against GTDB), either differential  
362 coverage or tetranucleotide frequency was used to identify and remove outlying contigs. The  
363 former was used for bins presenting a large variation in contig coverage across samples, and  
364 the latter for those that showed marked differences in GC content across contigs. Bins  $\geq 50\%$   
365 complete and  $\leq 10\%$  redundant were renamed as MAGs.

## 366 **Hybrid re-assembly**

367 Illumina and Nanopore bins were matched based on a 90% average nucleotide identity (ANI)  
368 threshold with fastANI<sup>75</sup> v1.3. Pairs of bins sharing  $\geq 90\%$  ANI were then subjected to a hybrid  
369 re-assembly approach with Unicycler<sup>76</sup> v0.4.8. For this, Illumina reads mapping to the  
370 respective Illumina and Nanopore bins were retrieved with SAMtools<sup>69</sup> v1.9 and seqtk<sup>60</sup> v1.3  
371 and assembled with SPAdes<sup>77</sup> v3.13.0. The SPAdes and Nanopore contigs were then assembled  
372 with miniasm<sup>78</sup> v0.3 and the resulting assembly was polished based on the Illumina reads with  
373 pilon<sup>70</sup> v1.23. Assemblies were processed with anvi'o as described above, with the exception that  
374 resulting bins were refined based on tetranucleotide frequency only.

## 375 **MAG dereplication and read recruitment analysis**

376 To remove redundancy (i.e. MAGs that were recovered multiple times across the different  
377 assemblies), Illumina and Nanopore MAGs were dereplicated based on a 90% ANI threshold  
378 with fastANI<sup>75</sup> v1.3. Non-redundant MAGs were replaced by their respective ‘hybrid’ MAG if  
379 the latter was of better quality (i.e. more complete, less redundant, with higher N<sub>50</sub> value, and/or  
380 included the 16S rRNA gene). Illumina reads were mapped to the set of non-redundant MAGs  
381 with bowtie<sup>68</sup> v2.3.5 and SAM files were sorted and indexed using SAMtools<sup>69</sup> v1.9. MAG  
382 detection and abundance was computed based on the nucleotide coverage across the Illumina  
383 reads. A MAG was considered detected in a given sample if  $\geq 50\%$  of its nucleotides had  $\geq 1x$   
384 coverage. Relative abundances were computed based on the number of reads recruited by each  
385 MAG normalised by the number of quality-filtered reads in each sample.

## 386 **MAG annotation**

387 Genome annotation was performed based on predicted amino acid sequences. Sequences were  
388 annotated against the COG database<sup>33</sup> release 12/2014 and the KEGG database<sup>34</sup> release 86  
389 with DIAMOND<sup>63</sup> v0.9.14, and the KOfam database<sup>35</sup> release 11/2020 with HMMER<sup>73</sup> v.3.2.1.  
390 A maximum e-value of  $10^{-5}$  was used for the DIAMOND-based annotations, and pre-computed  
391 family-specific thresholds were used for the HMMER-based annotation. Sequences assigned to  
392 denitrifying reductases were confirmed by similarity searches against the RefSeq<sup>36</sup> and Swiss-  
393 Prot databases using blastp<sup>79</sup> v2.9.0. Annotation of denitrifying reductases was also performed  
394 for previously published genomes retrieved from GenBank. These included a set of 1529 MAGs  
395 obtained from soils in Stordalen Mire, northern Sweden<sup>24</sup>, and all genomes of Acidobacteriota  
396 strains and candidate taxa.

## 397 **Phylogenomic analyses**

398 Phylogenetic assignment of MAGs was performed against the GTDB<sup>31,32</sup> release 05-RS95 based  
399 on 122 archaeal and 120 bacterial single-copy genes with GTDB-Tk<sup>80</sup> v1.3.0. Acidobacteriota  
400 MAGs encoding denitrifying reductases were submitted to further phylogenomic analyses  
401 alongside the genomes of Acidobacteriota strains and candidate taxa retrieved from GenBank.  
402 For this, the amino acid sequence of 23 ribosomal proteins was retrieved for each genome with  
403 anvio<sup>30</sup> v6.2 and aligned with MUSCLE<sup>81</sup> v3.8.1551. A maximum likelihood tree was then  
404 computed based on the concatenated alignments with FastTree<sup>82</sup> v2.1.10.

## 405 **Data availability**

406 Raw metagenomic data and assembled MAGs have been submitted to the European Nucleotide  
407 Archive (ENA) under the project PRJEB41762.

## 408 **Code availability**

409 All the code used can be found in <https://github.com/ArcticMicrobialEcology/Kilpisjarvi-MAGs>.

## 410 **References**

- 411 1. Tian, H. *et al.* A comprehensive quantification of global nitrous oxide sources and sinks.  
412 *Nature* **586**, 248–256 (2020).
- 413 2. Repo, M. E. *et al.* Large N<sub>2</sub>O emissions from cryoturbated peat soil in tundra. *Nat. Geosci.*  
414 **2**, 189–192 (2009).
- 415 3. Stewart, K. J., Grogan, P., Coxson, D. S. & Siciliano, S. D. Topography as a key factor driving  
416 atmospheric nitrogen exchanges in arctic terrestrial ecosystems. *Soil Biol. Biochem.* **70**,  
417 96–112 (2014).
- 418 4. Voigt, C. *et al.* Increased nitrous oxide emissions from Arctic peatlands after permafrost  
419 thaw. *Proc. Natl. Acad. Sci.* **114**, 6238–6243 (2017).
- 420 5. Voigt, C. *et al.* Nitrous oxide emissions from permafrost-affected soils. *Nat. Rev. Earth*  
421 *Environ.* **1**, 420–434 (2020).
- 422 6. Hugelius, G. *et al.* Large stocks of peatland carbon and nitrogen are vulnerable to  
423 permafrost thaw. *Proc. Natl. Acad. Sci.* **117**, 20438–20446 (2020).
- 424 7. Schuur, E. A. G. *et al.* Climate change and the permafrost carbon feedback. *Nature* **520**,  
425 171–179 (2015).
- 426 8. Post, E. *et al.* The polar regions in a 2°C warmer world. *Sci. Adv.* **5**, eaaw9883 (2019).
- 427 9. Butterbach-Bahl, K., Baggs, E. M., Dannenmann, M., Kiese, R. & Zechmeister-Boltenstern,  
428 S. Nitrous oxide emissions from soils: how well do we understand the processes and their  
429 controls? *Philos. Trans. R. Soc. B Biol. Sci.* **368**, 20130122 (2013).
- 430 10. Zumft, W. G. Cell biology and molecular basis of denitrification. *Microbiol. Mol. Biol. Rev.*  
431 **61**, 533–616 (1997).

- 432 11. Graf, D. R. H., Jones, C. M. & Hallin, S. Intergenomic comparisons highlight modularity of  
433 the denitrification pathway and underpin the importance of community structure for N<sub>2</sub>O  
434 emissions. *PLoS ONE* **9**, e114118 (2014).
- 435 12. Wallenstein, M. D., Myrold, D. D., Firestone, M. & Voytek, M. Environmental controls on  
436 denitrifying communities and denitrification rates: insights from molecular methods. *Ecol.*  
437 *Appl.* **16**, 2143–2152 (2006).
- 438 13. Kou, D. *et al.* Progressive nitrogen limitation across the Tibetan alpine permafrost region.  
439 *Nat. Commun.* **11**, 3331 (2020).
- 440 14. Liu, X.-Y. *et al.* Nitrate is an important nitrogen source for Arctic tundra plants. *Proc. Natl.*  
441 *Acad. Sci.* **115**, 3398–3403 (2018).
- 442 15. Yergeau, E., Kang, S., He, Z., Zhou, J. & Kowalchuk, G. A. Functional microarray analysis  
443 of nitrogen and carbon cycling genes across an Antarctic latitudinal transect. *ISME J.* **1**,  
444 163–179 (2007).
- 445 16. Yergeau, E., Hogues, H., Whyte, L. G. & Greer, C. W. The functional potential of high Arctic  
446 permafrost revealed by metagenomic sequencing, qPCR and microarray analyses. *ISME J.*  
447 **4**, 1206–1214 (2010).
- 448 17. Palmer, K., Biasi, C. & Horn, M. A. Contrasting denitrifier communities relate to  
449 contrasting N<sub>2</sub>O emission patterns from acidic peat soils in arctic tundra. *ISME J.* **6**,  
450 1058–1077 (2012).
- 451 18. Dai, H.-T., Zhu, R.-B., Sun, B.-W., Che, C.-S. & Hou, L.-J. Effects of sea animal activities on  
452 tundra soil denitrification and nirS- and nirK-encoding denitrifier community in Maritime  
453 Antarctica. *Front. Microbiol.* **11**, 573302 (2020).
- 454 19. Yu, T. & Zhuang, Q. Quantifying global N<sub>2</sub>O emissions from natural ecosystem soils using  
455 trait-based biogeochemistry models. *Biogeosciences* **16**, 207–222 (2019).
- 456 20. Rappé, M. S. & Giovannoni, S. J. The uncultured microbial majority. *Annu. Rev. Microbiol.*  
457 **57**, 369–394 (2003).
- 458 21. Steen, A. D. *et al.* High proportions of bacteria and archaea across most biomes remain  
459 uncultured. *ISME J.* **13**, 3126–3130 (2019).
- 460 22. Mackelprang, R. *et al.* Metagenomic analysis of a permafrost microbial community reveals  
461 a rapid response to thaw. *Nature* **480**, 368–371 (2011).
- 462 23. Hultman, J. *et al.* Multi-omics of permafrost, active layer and thermokarst bog soil  
463 microbiomes. *Nature* **521**, 208–212 (2015).



- 464 24. Woodcroft, B. J. *et al.* Genome-centric view of carbon processing in thawing permafrost.  
465 *Nature* **560**, 49–54 (2018).
- 466 25. le Roux, P. C., Aalto, J. & Luoto, M. Soil moisture’s underestimated role in climate change  
467 impact modelling in low-energy systems. *Glob. Change Biol.* **19**, 2965–2975 (2013).
- 468 26. Niittynen, P. *et al.* Fine-scale tundra vegetation patterns are strongly related to winter  
469 thermal conditions. *Nat. Clim. Change* **10**, 1143–1148 (2020).
- 470 27. Viitamäki, S. The activity and functions of soil microbial communities across a climate  
471 gradient in Finnish subarctic. Master’s thesis (University of Helsinki, 2019).
- 472 28. le Roux, P. C., Pellissier, L., Wisz, M. S. & Luoto, M. Incorporating dominant species as  
473 proxies for biotic interactions strengthens plant community models. *J. Ecol.* **102**, 767–775  
474 (2014).
- 475 29. Kemppinen, J., Niittynen, P., Aalto, J., le Roux, P. C. & Luoto, M. Water as a resource, stress  
476 and disturbance shaping tundra vegetation. *Oikos* **128**, 811–822 (2019).
- 477 30. Eren, A. M. *et al.* Anvi’o: an advanced analysis and visualization platform for ‘omics data.  
478 *PeerJ* **3**, e1319 (2015).
- 479 31. Parks, D. H. *et al.* A standardized bacterial taxonomy based on genome phylogeny  
480 substantially revises the tree of life. *Nat. Biotechnol.* **36**, 996–1004 (2018).
- 481 32. Parks, D. H. *et al.* A complete domain-to-species taxonomy for Bacteria and Archaea. *Nat.*  
482 *Biotechnol.* **38**, 1079–1086 (2020).
- 483 33. Galperin, M. Y., Makarova, K. S., Wolf, Y. I. & Koonin, E. V. Expanded microbial genome  
484 coverage and improved protein family annotation in the COG database. *Nucleic Acids Res.*  
485 **43**, D261–D269 (2015).
- 486 34. Kanehisa, M. KEGG: Kyoto Encyclopedia of Genes and Genomes. *Nucleic Acids Res.* **28**,  
487 27–30 (2000).
- 488 35. Aramaki, T. *et al.* KofamKOALA: KEGG Ortholog assignment based on profile HMM and  
489 adaptive score threshold. *Bioinformatics* **36**, 2251–2252 (2020).
- 490 36. O’Leary, N. A. *et al.* Reference sequence (RefSeq) database at NCBI: current status,  
491 taxonomic expansion, and functional annotation. *Nucleic Acids Res.* **44**, D733–D745 (2016).
- 492 37. The UniProt Consortium. UniProt: a worldwide hub of protein knowledge. *Nucleic Acids*  
493 *Res.* **47**, D506–D515 (2019).

- 494 38. Delgado-Baquerizo, M. *et al.* A global atlas of the dominant bacteria found in soil. *Science*  
495 **359**, 320–325 (2018).
- 496 39. Shiro, Y. Structure and function of bacterial nitric oxide reductases. *Biochim. Biophys. Acta*  
497 *- Bioenerg.* **1817**, 1907–1913 (2012).
- 498 40. Männistö, M. K., Kurhela, E., Tirola, M. & Häggblom, M. M. Acidobacteria dominate the  
499 active bacterial communities of Arctic tundra with widely divergent winter-time snow  
500 accumulation and soil temperatures. *FEMS Microbiol. Ecol.* **84**, 47–59 (2013).
- 501 41. Kalam, S. *et al.* Recent understanding of soil Acidobacteria and their ecological significance:  
502 a critical review. *Front. Microbiol.* **11**, 580024 (2020).
- 503 42. Jones, C. M., Stres, B., Rosenquist, M. & Hallin, S. Phylogenetic analysis of nitrite, nitric  
504 oxide, and nitrous oxide respiratory enzymes reveal a complex evolutionary history for  
505 denitrification. *Mol. Biol. Evol.* **25**, 1955–1966 (2008).
- 506 43. Sanford, R. A. *et al.* Unexpected nondenitrifier nitrous oxide reductase gene diversity and  
507 abundance in soils. *Proc. Natl. Acad. Sci.* **109**, 19709–19714 (2012).
- 508 44. Ortiz, M. *et al.* Microbial nitrogen cycling in Antarctic soils. *Microorganisms* **8**, 1442 (2020).
- 509 45. Makhalanyane, T. P., Van Goethem, M. W. & Cowan, D. A. Microbial diversity and  
510 functional capacity in polar soils. *Curr. Opin. Biotechnol.* **38**, 159–166 (2016).
- 511 46. Kielak, A. M., Barreto, C. C., Kowalchuk, G. A., van Veen, J. A. & Kuramae, E. E. The  
512 ecology of Acidobacteria: moving beyond genes and genomes. *Front. Microbiol.* **7**, (2016).
- 513 47. Eichorst, S. A. *et al.* Genomic insights into the Acidobacteria reveal strategies for their  
514 success in terrestrial environments. *Environ. Microbiol.* **20**, 1041–1063 (2018).
- 515 48. Lycus, P. *et al.* Phenotypic and genotypic richness of denitrifiers revealed by a novel isolation  
516 strategy. *ISME J.* **11**, 2219–2232 (2017).
- 517 49. Philippot, L., Andert, J., Jones, C. M., Bru, D. & Hallin, S. Importance of denitrifiers lacking  
518 the genes encoding the nitrous oxide reductase for N<sub>2</sub>O emissions from soil. *Glob. Change*  
519 *Biol.* **17**, 1497–1504 (2011).
- 520 50. Jones, C. M. *et al.* Recently identified microbial guild mediates soil N<sub>2</sub>O sink capacity. *Nat.*  
521 *Clim. Change* **4**, 801–805 (2014).
- 522 51. Jones, C. M., Graf, D. R., Bru, D., Philippot, L. & Hallin, S. The unaccounted yet abundant  
523 nitrous oxide-reducing microbial community: a potential nitrous oxide sink. *ISME J.* **7**, 417–  
524 426 (2013).

- 525 52. Schimel, J. Microbial ecology: Linking omics to biogeochemistry. *Nat. Microbiol.* **1**, 15028  
526 (2016).
- 527 53. Bakken, L. R., Bergaust, L., Liu, B. & Frostegård, Å. Regulation of denitrification at the  
528 cellular level: a clue to the understanding of N<sub>2</sub>O emissions from soils. *Philos. Trans. R. Soc.*  
529 *B Biol. Sci.* **367**, 1226–1234 (2012).
- 530 54. Pirinen, P. *et al.* *Climatological statistics of Finland 1981–2010*. (Finnish Meteorological  
531 Institute, 2012).
- 532 55. Andrews, S. *FastQC: A Quality Control Tool for High Throughput Sequence Data*. (2019).  
533 Available at <https://www.bioinformatics.babraham.ac.uk/projects/fastqc>.
- 534 56. Ewels, P., Magnusson, M., Lundin, S. & Käller, M. MultiQC: summarize analysis results for  
535 multiple tools and samples in a single report. *Bioinformatics* **32**, 3047–3048 (2016).
- 536 57. Martin, M. Cutadapt removes adapter sequences from high-throughput sequencing reads.  
537 *EMBnet.journal* **17**, 10 (2011).
- 538 58. Leger, A. & Leonardi, T. pycoQC, interactive quality control for Oxford Nanopore  
539 Sequencing. *J. Open Source Softw.* **4**, 1236 (2019).
- 540 59. Wick, R. R. *Porechop*. (2018). Available at <https://github.com/rrwick/Porechop>.
- 541 60. Li, H. *seqtk*. (2018). Available at <https://github.com/lh3/seqtk>.
- 542 61. Quast, C. *et al.* The SILVA ribosomal RNA gene database project: improved data processing  
543 and web-based tools. *Nucleic Acids Res.* **41**, D590–D596 (2012).
- 544 62. Bengtsson-Palme, J. *et al.* METAXA 2: improved identification and taxonomic classification  
545 of small and large subunit rRNA in metagenomic data. *Mol. Ecol. Resour.* **15**, 1403–1414  
546 (2015).
- 547 63. Buchfink, B., Xie, C. & Huson, D. H. Fast and sensitive protein alignment using DIAMOND.  
548 *Nat. Methods* **12**, 59–60 (2015).
- 549 64. Pessi, I. S. *keggR*. (2020). Available at <https://github.com/igorspp/keggR>.
- 550 65. Oksanen, J. *et al.* *vegan: community ecology package*. (2019). Available at [https://cran.r-](https://cran.r-project.org/web/packages/vegan)  
551 [project.org/web/packages/vegan](https://cran.r-project.org/web/packages/vegan).
- 552 66. Li, D., Liu, C.-M., Luo, R., Sadakane, K. & Lam, T.-W. MEGAHIT: an ultra-fast single-node  
553 solution for large and complex metagenomics assembly via succinct de Bruijn graph.  
554 *Bioinformatics* **31**, 1674–1676 (2015).

- 555 67. Kolmogorov, M. *et al.* metaFlye: scalable long-read metagenome assembly using repeat  
556 graphs. *Nat. Methods* **17**, 1103–1110 (2020).
- 557 68. Langmead, B. & Salzberg, S. L. Fast gapped-read alignment with Bowtie 2. *Nat. Methods*  
558 **9**, 357–359 (2012).
- 559 69. Li, H. *et al.* The Sequence Alignment/Map format and SAMtools. *Bioinformatics* **25**, 2078–  
560 2079 (2009).
- 561 70. Walker, B. J. *et al.* Pilon: an integrated tool for comprehensive microbial variant detection  
562 and genome assembly improvement. *PLoS ONE* **9**, e112963 (2014).
- 563 71. Mikheenko, A., Saveliev, V. & Gurevich, A. MetaQUAST: evaluation of metagenome  
564 assemblies. *Bioinformatics* **32**, 1088–1090 (2016).
- 565 72. Hyatt, D. *et al.* Prodigal: prokaryotic gene recognition and translation initiation site  
566 identification. *BMC Bioinformatics* **11**, 119 (2010).
- 567 73. Eddy, S. R. Accelerated profile HMM searches. *PLoS Comput. Biol.* **7**, e1002195 (2011).
- 568 74. Alneberg, J. *et al.* Binning metagenomic contigs by coverage and composition. *Nat. Methods*  
569 **11**, 1144–1146 (2014).
- 570 75. Jain, C., Rodriguez-R, L. M., Phillippy, A. M., Konstantinidis, K. T. & Aluru, S. High  
571 throughput ANI analysis of 90K prokaryotic genomes reveals clear species boundaries. *Nat.*  
572 *Commun.* **9**, 5114 (2018).
- 573 76. Wick, R. R., Judd, L. M., Gorrie, C. L. & Holt, K. E. Unicycler: resolving bacterial genome  
574 assemblies from short and long sequencing reads. *PLOS Comput. Biol.* **13**, e1005595 (2017).
- 575 77. Bankevich, A. *et al.* SPAdes: A new genome assembly algorithm and its applications to  
576 single-cell sequencing. *J. Comput. Biol.* **19**, 455–477 (2012).
- 577 78. Li, H. Minimap and miniasm: fast mapping and de novo assembly for noisy long sequences.  
578 *Bioinformatics* **32**, 2103–2110 (2016).
- 579 79. Camacho, C. *et al.* BLAST+: architecture and applications. *BMC Bioinformatics* **10**, 421  
580 (2009).
- 581 80. Chaumeil, P.-A., Mussig, A. J., Hugenholtz, P. & Parks, D. H. GTDB-Tk: a toolkit to classify  
582 genomes with the Genome Taxonomy Database. *Bioinformatics* **36**, 1925–1927 (2019).
- 583 81. Edgar, R. C. MUSCLE: multiple sequence alignment with high accuracy and high  
584 throughput. *Nucleic Acids Res.* **32**, 1792–1797 (2004).

585 82. Price, M. N., Dehal, P. S. & Arkin, A. P. FastTree 2 – approximately maximum-likelihood  
586 trees for large alignments. *PLoS ONE* **5**, e9490 (2010).

## 587 **Acknowledgements**

588 This work was funded by the Academy of Finland (grants 314114 and 335354) and the  
589 University of Helsinki. SV was funded by the Microbiology and Biotechnology Doctoral  
590 Programme (MBDP). We would like to acknowledge the CSC – IT Centre for Science for  
591 providing the requisite computing resources and Mr. Kimmo Mattila for IT support; the staff  
592 from the Kilpisjärvi Biological Station, Tanja Orpana, Aino Rutanen, Anniina Sarekoski, Anna-  
593 Maria Virkkala, and Miska Luoto’s group members for assistance with fieldwork and soil  
594 characterization; Christina Biasi and Maija Marushchak for helpful discussion; Laura  
595 Cappelatti for revising the manuscript and assistance with figures; and Murat Eren, Sebastian  
596 Lücker, Donovan Parks, and Antonios Kioukis for tips, recommendations, and troubleshooting  
597 regarding the bioinformatics analyses.

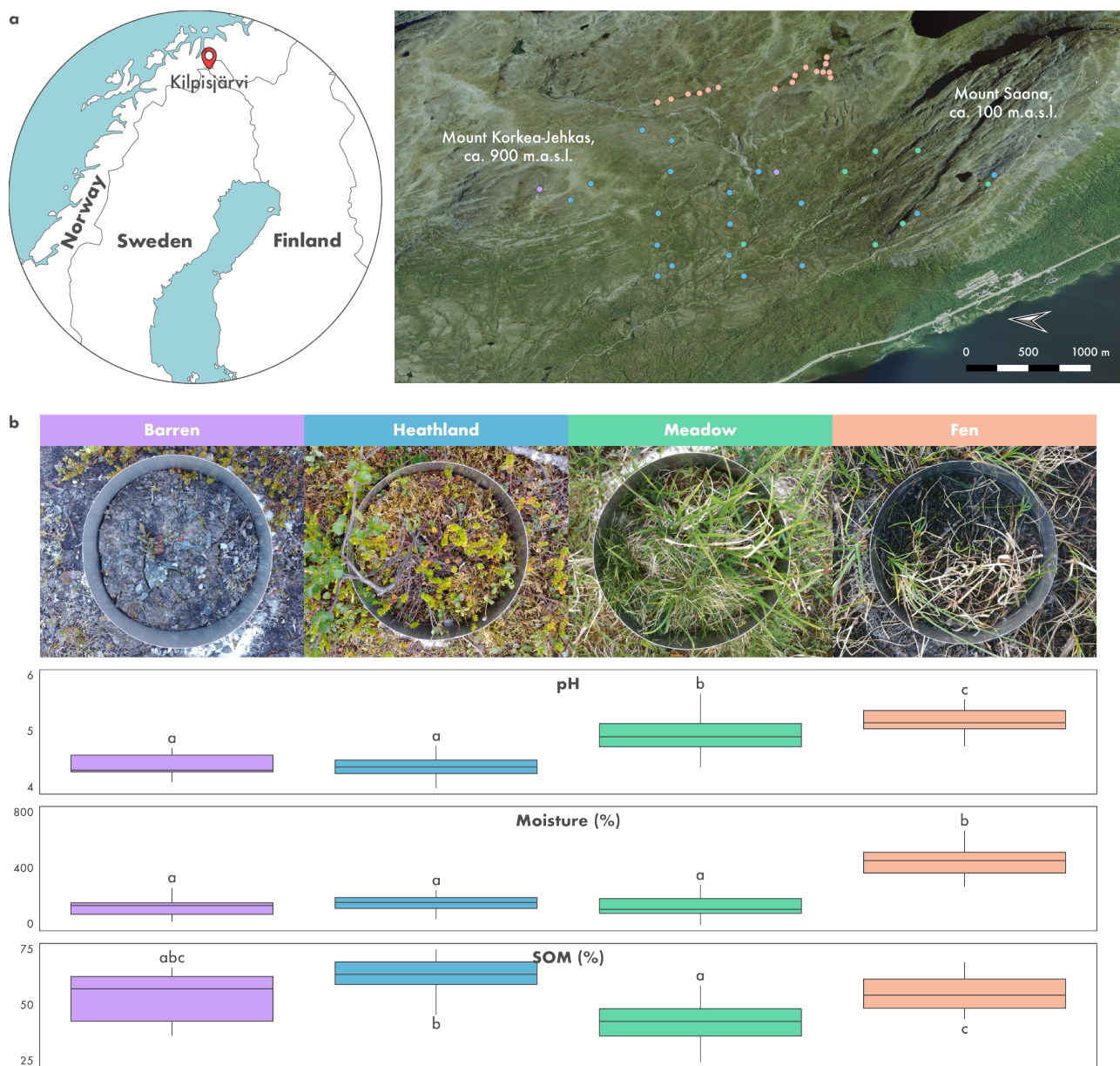
## 598 **Author contributions**

599 JH and ML designed the research; SV and JH performed nucleic acid extraction and library  
600 preparation; ISP analysed the data and wrote the manuscript; EER and TOD contributed with  
601 the analyses; all authors contributed to the final version of the manuscript.

## 602 **Competing interests**

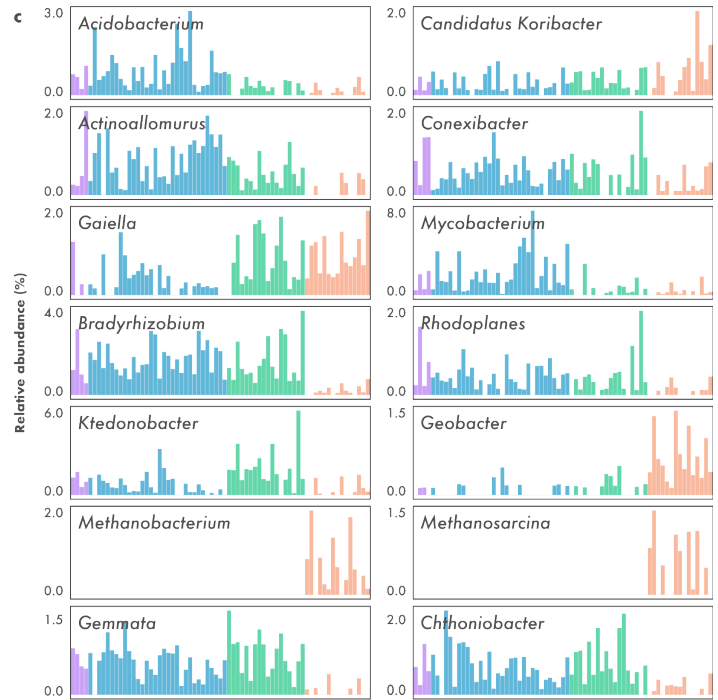
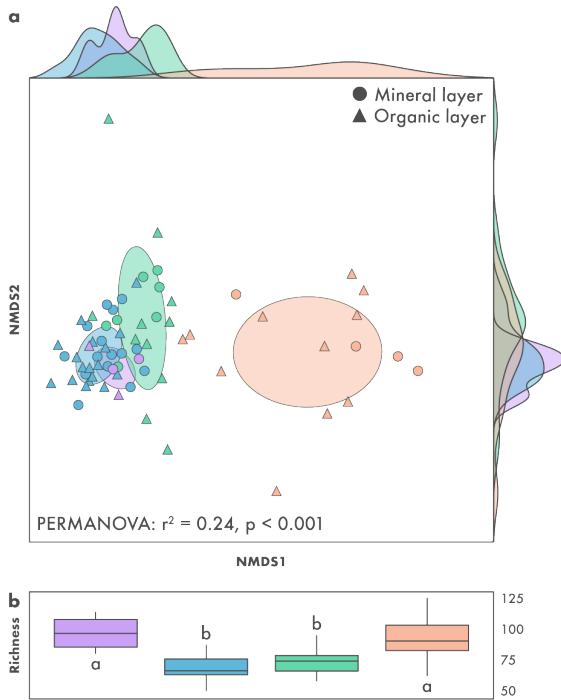
603 The authors declare no competing interests.

604 **Supplementary Figures**

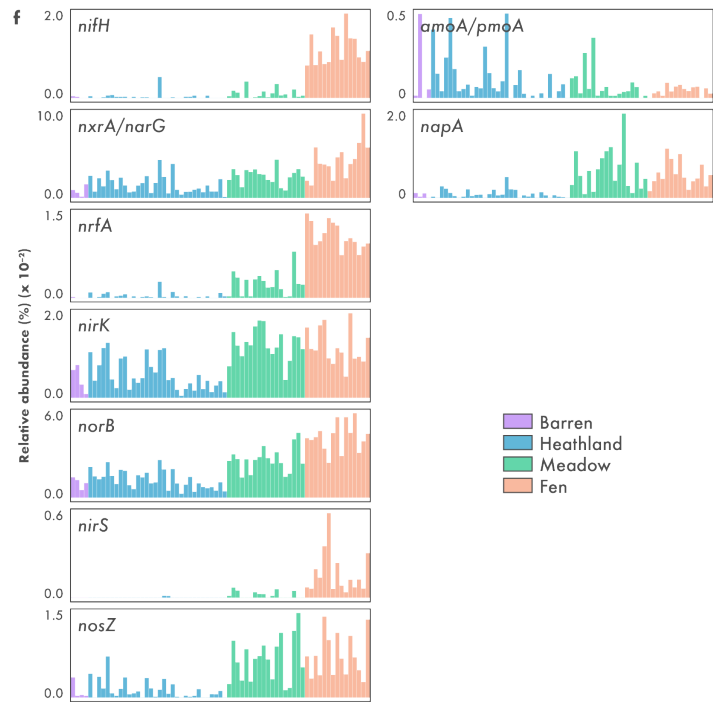
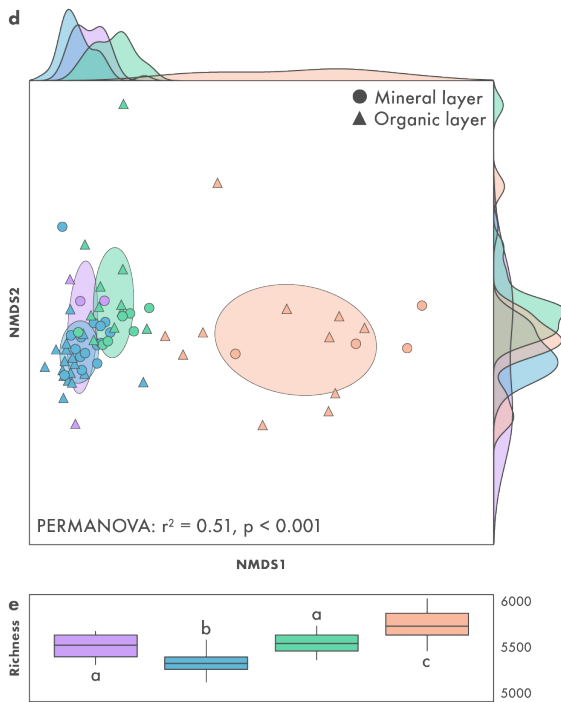


605 **Suppl. Fig. S1 | Saana Nature Reserve, an area of mountain tundra in Kilpisjärvi,**  
606 **northern Finland. a)** Map of Fennoscandia showing the location of Kilpisjärvi and topographic  
607 overview of the study area. **b)** Characterization of the four types of soil ecosystems investigated.  
608 Ecosystems that do not share the same letter are significantly different (one-way ANOVA  
609 followed by Tukey's HSD test;  $p < 0.001$ ).

### Taxonomic composition (genus level)

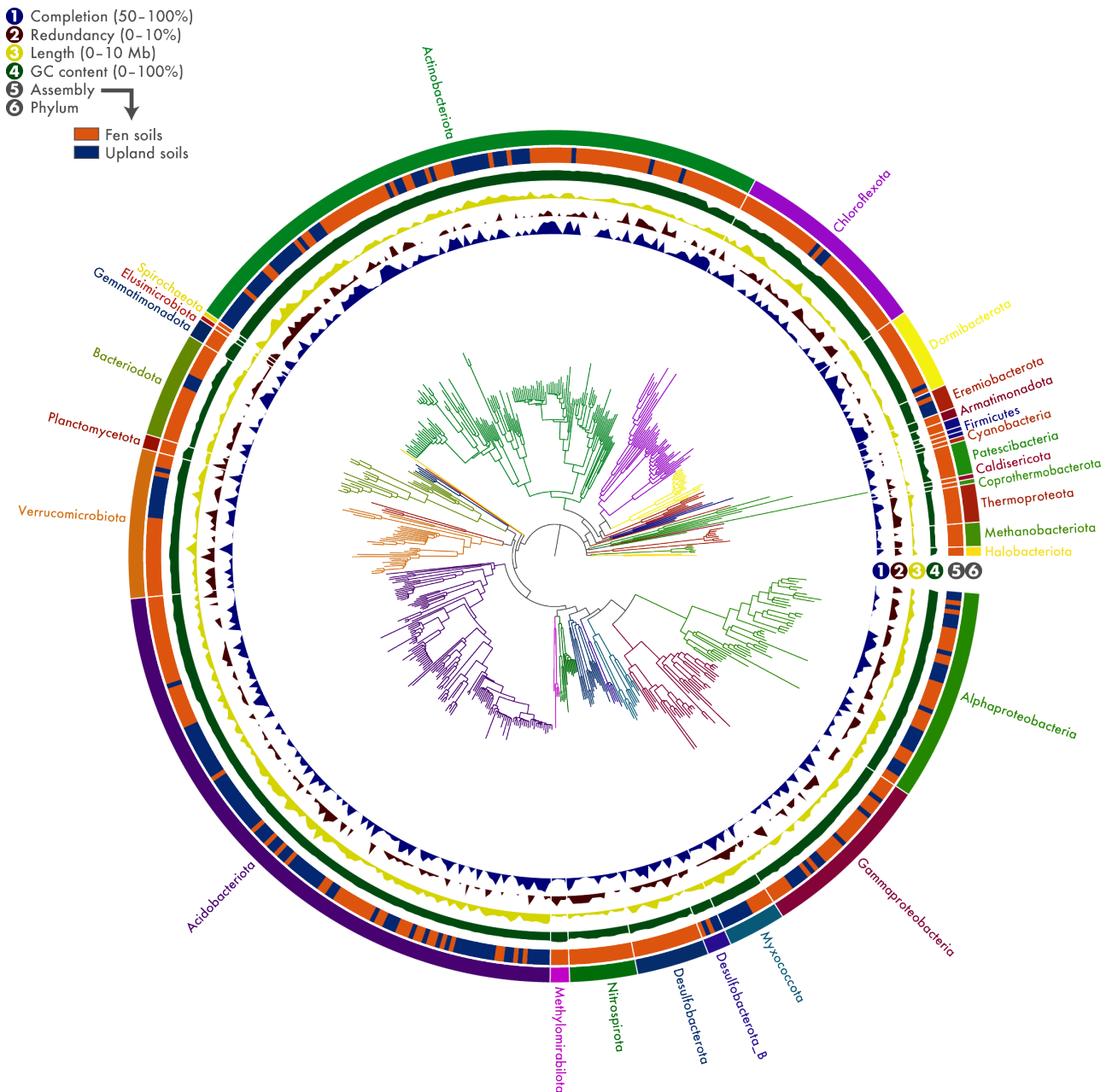


### Functional composition

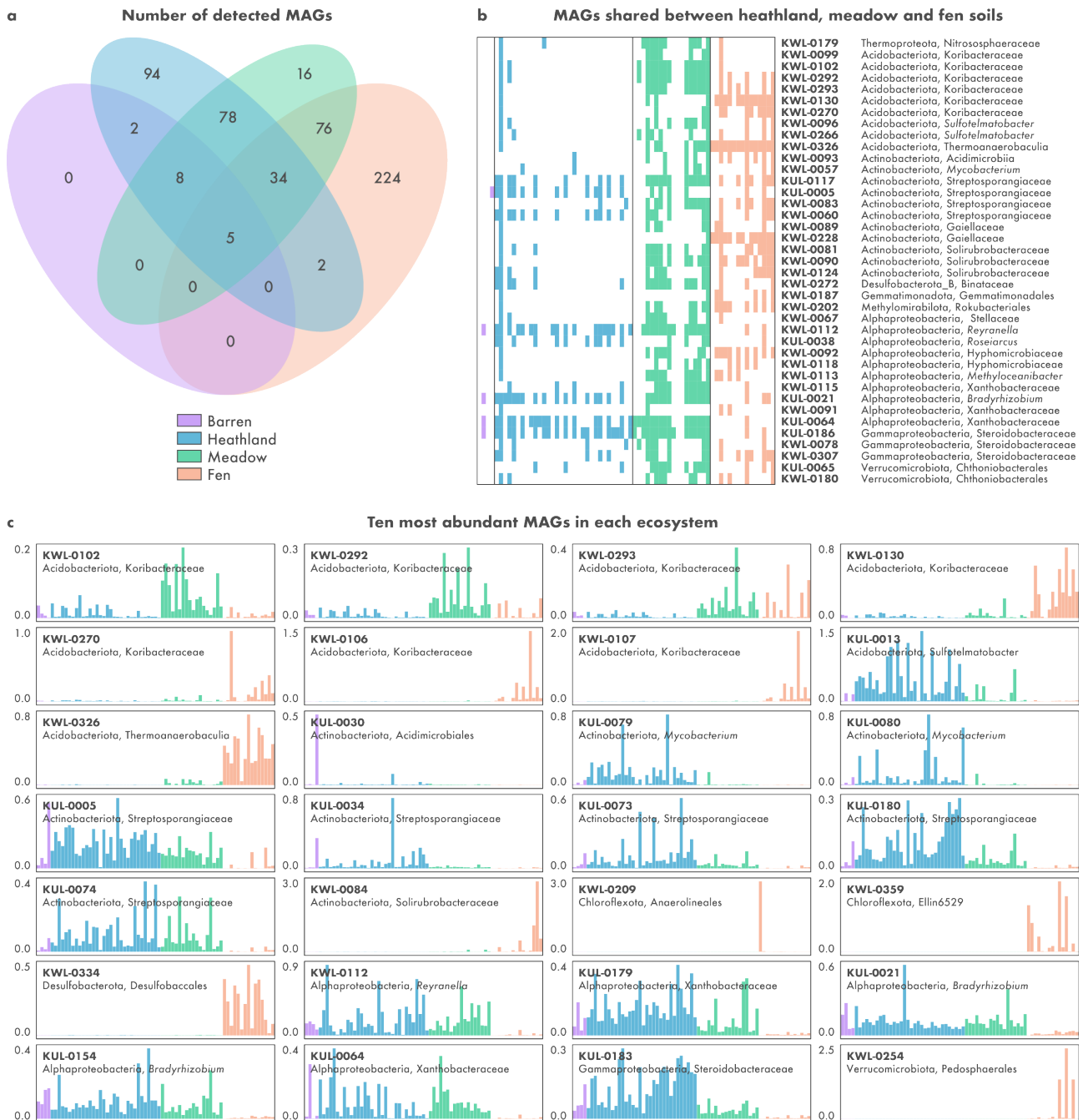


610 **(Previous page) Suppl. Fig. S2 | The microbial diversity of Kilpisjärvi soils as seen**  
611 **using a gene-centric approach.** Gene-centric analyses were carried out using unassembled  
612 Illumina data. Taxonomic composition was computed based on the annotation of 16S rRNA gene  
613 fragments against the SILVA database<sup>61</sup> with METAXA<sup>62</sup>. Functional annotation was  
614 performed by blastx searches against the KEGG database<sup>34</sup> with DIAMOND<sup>63</sup>. **a, d)** Non-metric  
615 multidimensional scaling (NMDS) of taxonomic and functional community structure.  
616 Differences between the ecosystems were assessed using permutational ANOVA  
617 (PERMANOVA). **b, e)** Taxonomic and functional richness (number of genera and functional  
618 genes). Differences in richness were assessed using one-way ANOVA followed by Tukey's HSD  
619 test. Ecosystems that do not share the same letter are significantly different ( $p < 0.001$ ).  
620 **c, f)** Abundance profile of the five most abundant genera in each ecosystem and marker genes  
621 for the different steps of the N cycle.

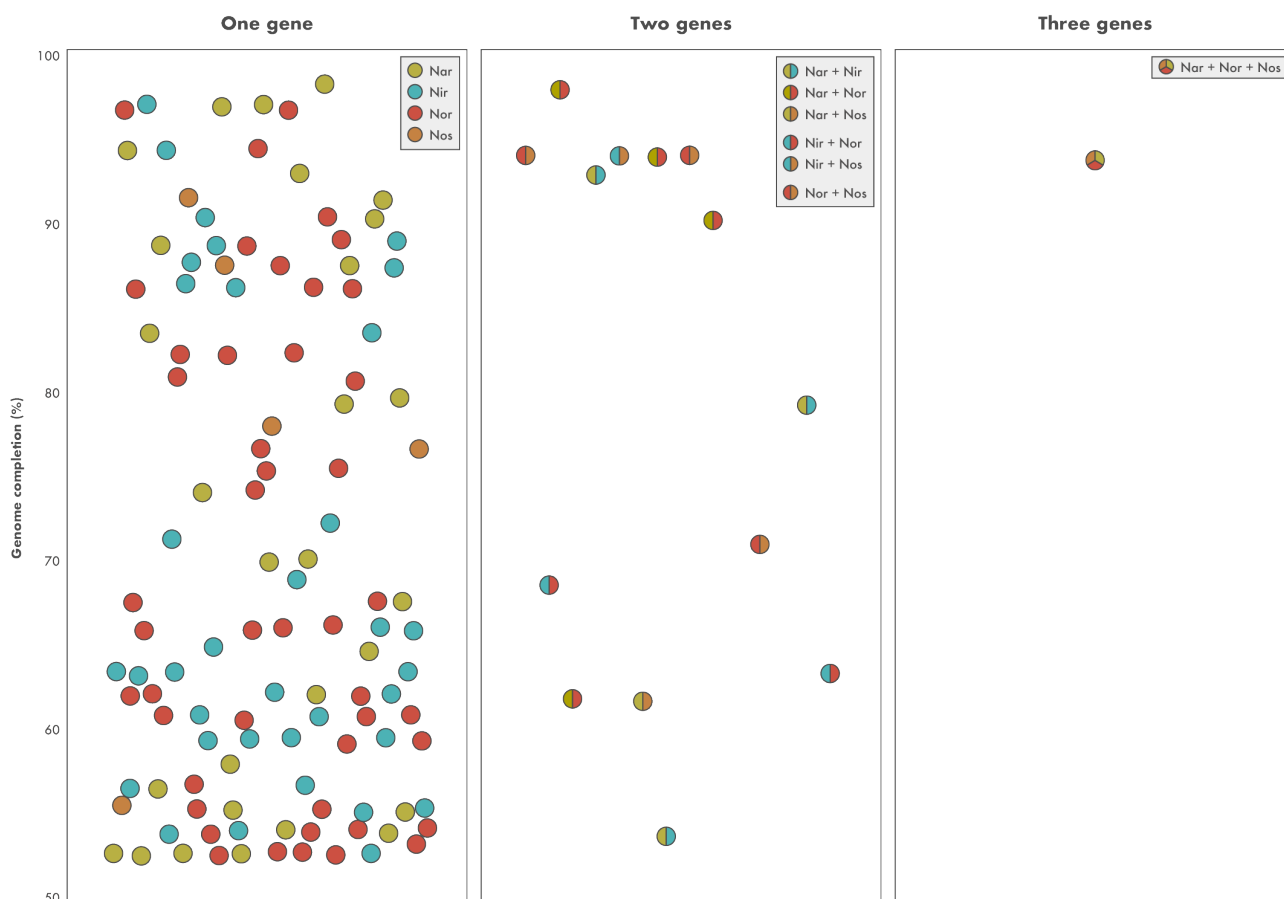




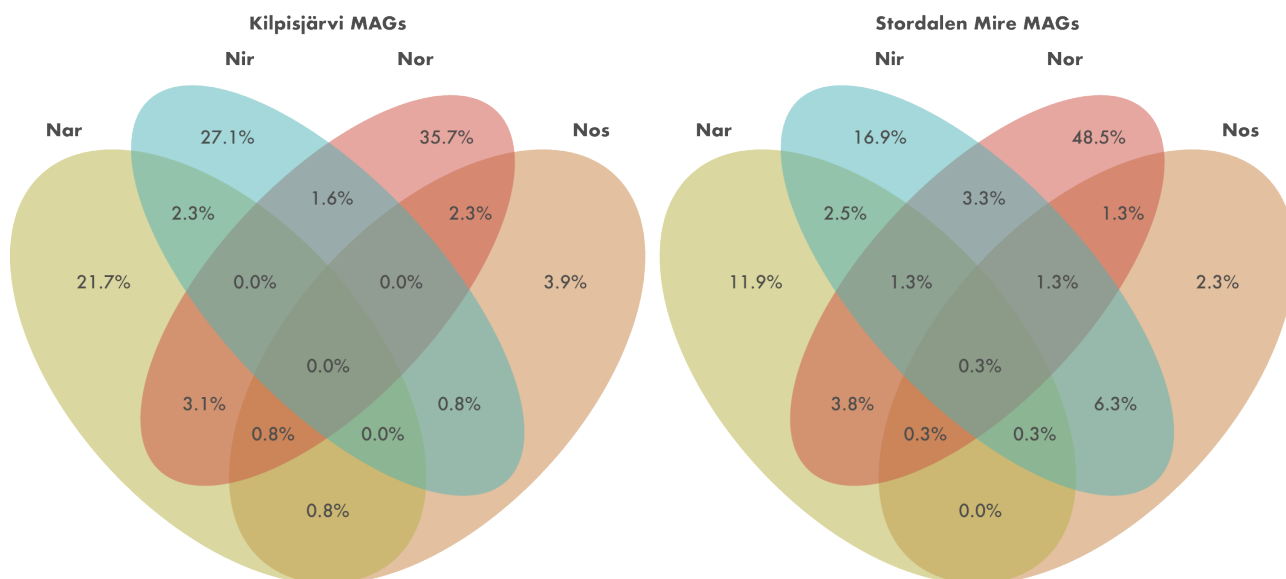
622 **Suppl. Fig. S3 | Five hundred thirty-nine metagenome assembled genomes (MAGs)**  
623 **from tundra soils.** Phylogenomic analysis of Kilpisjärvi MAGs based on concatenated  
624 alignments of amino acid sequences from 122 archaeal and 120 bacterial single-copy genes.  
625 MAGs completion and redundancy were computed based on the presence of single-copy genes.



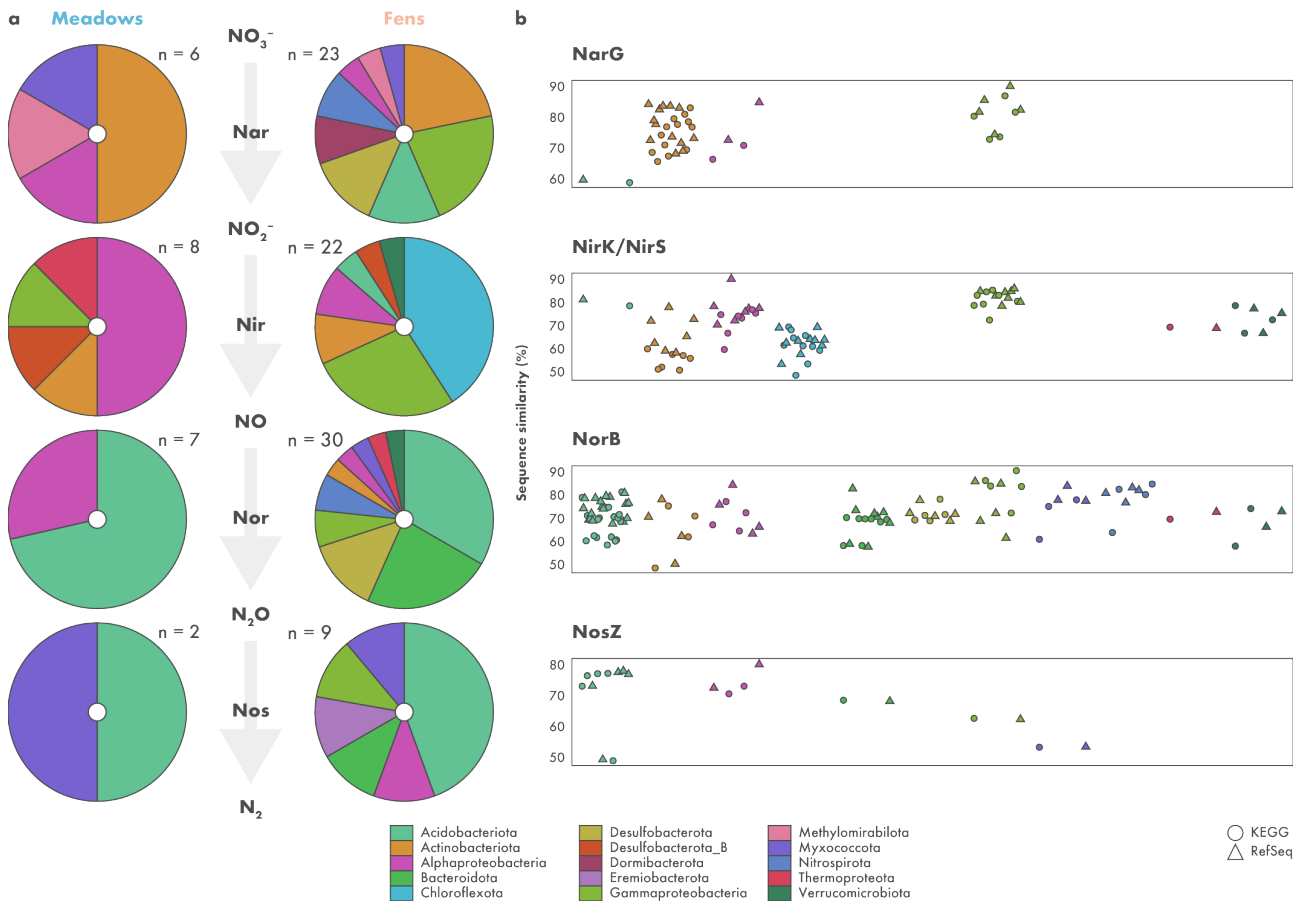
626 **Suppl. Fig. S4 | Overview of the microbial diversity of Kilpisjärvi soils based on a**  
 627 **genome- resolved approach. a) Number of detected MAGs across the ecosystems. A MAG**  
 628 **was detected in a given sample if  $\geq 50\%$  of its nucleotides had  $\geq 1x$  coverage. b) Detection profiles**  
 629 **of MAGs shared between heathland, meadow, and fen soils. c) Relative abundance of the ten**  
 630 **most abundant MAGs in each ecosystem.**



631 **Suppl. Fig. S5 | Relationship between MAG completion and number of denitrifying**  
632 **reductases.** MAGs completion was computed based on the presence of single-copy genes. The  
633 presence of nitrate (Nar), nitrite (Nir), nitric oxide (Nor), and nitrous oxide (Nos) reductases  
634 was inferred based on the annotation of predicted amino acid sequences.



635 **Suppl. Fig. S6 | Percentage of MAGs encoding denitrifying reductases in Kilpisjärvi**  
636 **and Stordalen Mire soils.** The presence of nitrate (Nar), nitrite (Nir), nitric oxide (Nor), and  
637 nitrous oxide (Nos) reductases was inferred based on the annotation of predicted amino acid  
638 sequences.



639 **Suppl. Fig. S7 | Community structure and identity of NarG, NirK/NirS, NorB, and**  
 640 **NosZ sequences. a) Taxonomic assignment of MAGs encoding each of the denitrifying**  
 641 **reductases in meadow and fen soils. b) Sequence similarity of denitrifying reductases encoded**  
 642 **by the MAGs with reference sequences in the KEGG and RefSeq databases.**